Using Open-Source Software Defined Radio Platforms for Empirical Characterization of Man-Made Impulsive Noise

Otilia Popescu, Senior Member, IEEE; John Musson; and Dimitrie C. Popescu, Senior Member, IEEE

Abstract—The paper discusses the use of affordable software-defined radio (SDR) platforms for measuring and characterizing man-made noise with impulsive components using Middleton noise models. For illustration, numerical results from a case study are presented, in which man-made noise is measured at three different locations corresponding to three distinct types of radio-frequency (RF) environments, and for which the parameters of the underlying Middleton Class A impulsive noise model are derived. The study demonstrates one of the many applications of SDR platforms, whose versatility enables dedicated noise measurements systems that can be configured through software.

Index Terms—Software Defined Radio, Impulsive Noise.

I. Introduction

Noise modeling is an important component in analyzing and designing communication systems, and in many instances, it is assumed that noise corrupting desired communication signals can be modeled as a Gaussian noise process. This assumption is accurate in the case of satellite and space communications, where thermal noise is dominant while other sources of noise and interference can be neglected. However, in the case of terrestrial communication systems, noise includes coherent and incoherent combinations of man-made signals that can exceed the thermal noise power by several orders of magnitude and can be observed by taking power measurements of background noise. In addition, impulsive noise caused by both human activities and natural phenomena can also affect desired signals in terrestrial communication systems. We note that, man-made impulsive noise can be due to intentional intelligible information exchange such as short-burst transmissions with high power, as well as due to unintelligible traces of switching and industrial activities, corona discharge of high voltage distribution lines, or automotive electronics [1], while impulsive noise that occurs naturally may be due to atmospheric phenomena such as lightning, meteorite activity, and spontaneous discharges in the atmosphere [2].

Noise measurements performed during the 1960 years were aimed at modeling atmospheric noise and used a combination of sophisticated ground-based equipment and airborne receivers, which required significant equipment rack space and heavy-duty power supplies [3], [4]. About two decades later advances in battery and inverter technology enabled mobile automotive platforms for noise measurement that required a fairly large vehicle to carry all signal generation and noise measurement equipment [5].

Today, miniaturization of integrated circuits and the expansion of software-defined electronics [6] make possible noise measurement systems that can be hand-carried within buildings, on industrial campuses, and remote locations. Using versatile SDR platforms [7] such as the Lime SDR from Lime Microsystems [8], the HackRF SDR from Great Scott Gadgets [9], or the USRP SDR by Ettus Research [10], along with a laptop computer with average computing capabilities and driven by open-source software, a powerful noise measurement system can be easily put together at a cost that is accessible to students and hobbyists.

In this paper we present the use of a Lime SDR platform from Lime Microsystems [8] to collect measurements of man-made noise with impulsive components in various RF environments, and we discuss how the collected data is processed to extract information on noise characteristics. The measured noise is described by Class A type impulsive noise Middleton models [11]–[13], for which their characteristics (the impulsive and intensity indices) are estimated from the collected data for three types of RF environments: one corresponding to a typical office space, one corresponding to a hospital campus, and a third one corresponding to a busy outdoor commuting environment. We note that part of this work has been presented in a concise format at the 14th IEEE International Symposium on Signals, Circuits, and Systems [14], and that the paper includes complete details of the work. Specifically, while reference [14] introduces only briefly the SDR setup for noise measurement and includes limited details on its processing with partial numerical results, the current paper includes full details on the measurement setup and of the processing required to obtain the time evolution of the Middleton parameters for the three scenarios for which measurements have been recorded.

The paper is organized as follows: we briefly review impulsive noise modeling in Section II with focus on the parameters that characterize the Class A Middleton impulsive noise model. We continue with presentation of the noise measurement setup in Section III that collects noise data using the Lime SDR platform. In Section IV we present the numerical results obtained for three distinct RF scenarios: a medium-density office workspace environment, an urban commute scenario, and a hospital campus. The paper is concluded with final remarks in Section V.

Otilia Popescu is with the Department of Engineering Technology, Old Dominion University, 102 Kaufman Hall, Norfolk, VA 23529. E-mail: opopescu@odu.edu.
John Musson is with the Engineering Division, Thomas Jefferson National Accelerator Facility, Newport News, VA 23606. E-mail: musson@jlab.org
Dimitrie C. Popescu is with the Department of Electrical and Computer Engineering, Old Dominion University, 231 Kaufman Hall, Norfolk, VA 23529. E-mail: dpopescu@odu.edu.

II. Modeling Noise with Impulsive Components

The complex-valued lowpass equivalent waveform z(t) that models noise with impulsive components in a RF band of interest consists of a sum of independent stochastic processes and includes a zero-mean complex-valued Gaussian process along with a superposition of narrowband impulses occurring in the same band at random time instances [1]. For empirical characterization, statistical detectors are used to collect measurements of the in-phase (I) and quadrature (Q) components of the noise, which are used to determine the noise root mean-squared (RMS) value and its corresponding magnitude in order to evaluate the power of the noise over a measurement window. The detectors include threshold sensing to identify specific events such as the RMS value of the noise or the noise power exceeding particular values that are usually related to the noise floor or the RMS measured value of the noise power in the absence of desired communication signals.

For illustration we present a snapshot of the power profile of a noise process with impulsive components in Fig. 1, which was obtained by taking measurements in the 137 MHz amateur radio band using a radio receiver with RF front-end bandwidth of 250 kHz [5]. As can be seen from Fig. 1, while the measured thermal noise floor fluctuates around –110 dBm[1], multiple impulses with short durations and powers exceeding the thermal noise floor by as much as 40 dB are recorded over the observation interval.

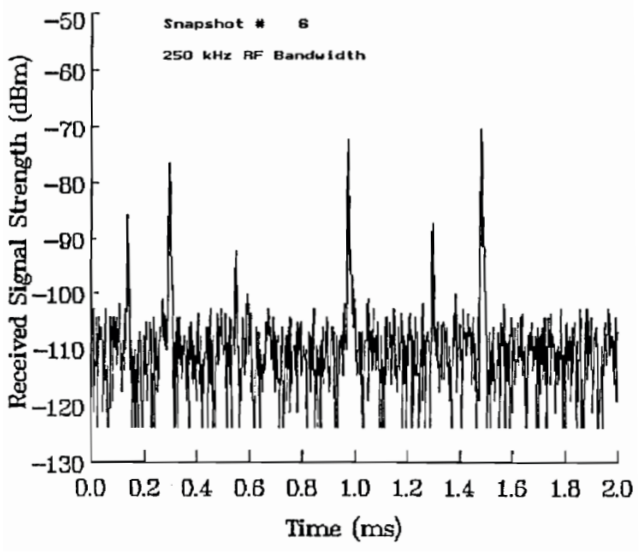

Fig. 1. Example of measured power profile for bandpass background noise process with impulsive components generated by a power plant on the Virginia Tech campus [5].

Analytical characterization of z(t) uses the statistical physical models developed by Middleton during the 1970s [15], [16] that distinguish between class A and class B impulsive noise processes, such that for a class A impulsive noise process z(t) the probability density function (PDF) is given by [16]:

$$p(z) = e^{A} \sum_{m=0}^{\infty} \frac{A^m}{m!} \frac{z}{\sigma_m^2} e^{-\frac{z^2}{2\sigma_m^2}} \qquad (1)$$

where $\sigma_m^2 = (m/A + \Gamma) / (1 + \Gamma)$, with denoting the impulsive noise index and Γ the intensity index. The impulsive index A provides an aggregate description of the impulsive events in terms of their rate and their duration, with small values of A indicating highly impulsive noise. The intensity index Γ describes the ratio of Gaussian to non-Gaussian components in the impulsive noise, with small values of Γ indicating significant contributions from impulsive processes.

The amplitude probability distribution (APD) for Class A impulsive noise is then given by [16]:

$$\mathrm{APD}(z_i) = \mathrm{Prob}[z(t) > z_i] = e^{-A} \sum_{m=0}^{\infty} \frac{A^m}{m!} e^{-\frac{z^2}{2\sigma_m^2}} \qquad (2)$$

Fig. 2 and 3 illustrate the PDF and APD, respectively, obtained using statistical detectors for the impulsive noise process with power profile illustrated in Fig. 1 [5]. We note that the step-like structure in the APD indicates the presence of signal levels consisting of specific amplitudes, and that the indices A and Γ of the impulsive noise process can be determined from the empirical data using the approach in [13].

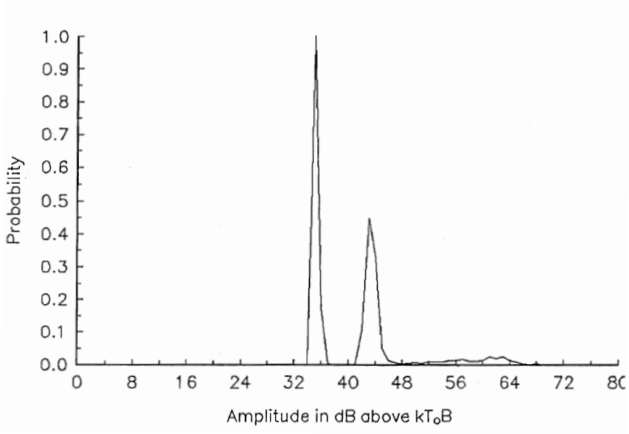

Fig. 2. PDF for the impulsive noise process with measured power profile shown in Fig. 1 [5].

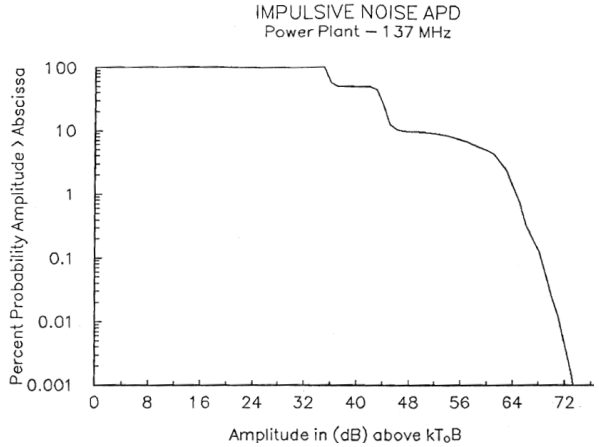

Fig. 3. APD corresponding to the impulsive noise process with measured power profile shown in Fig. 1 [5].

[1] The analytical expression of the thermal noise floor is kT_0B, where k is Boltzmann's constant, T_0 = 290 K, and B is the width of the RF band of interest. For B = 250 kHz the theoretical noise floor value is –120 dBm.

Fig. 4. Full size van converted into a mobile platform to perform impulsive noise measurements in the early 1990s [5]. Power equipment was located in the back area of the van.

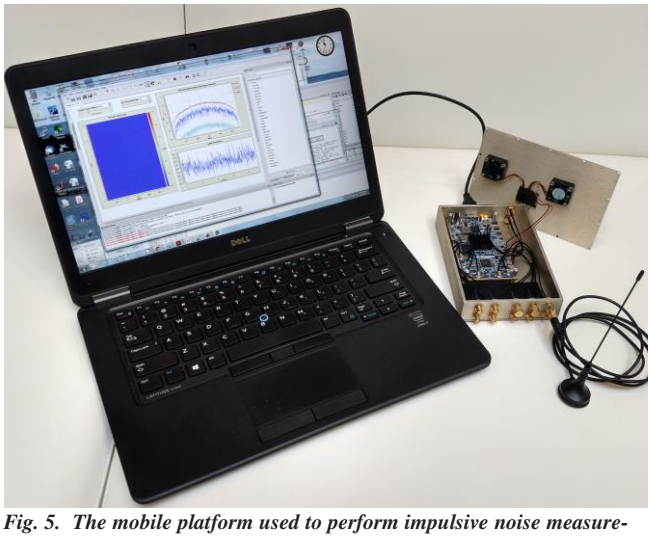

Fig. 5. The mobile platform used to perform impulsive noise measurements presented in the paper. The Lime SDR board is mounted inside a custom aluminum enclosure and is used in conjunction with a 900 MHz monopole antenna connected to the RX1_L input of the board.

III. SDR Setup for Measuring Impulsive Noise

The items needed to perform an empirical characterization of impulsive noise include a radio receiver, a spectrum analyzer, a logarithmic detector, a digital oscilloscope, and a computer. We note that performing a similar noise characterization study as the one presented in this paper during the early 1990s required access to a well-equipped lab dedicated to communication systems where all the items, which had significant price tags at the time, were available [5]. Furthermore, in order to incorporate this equipment into a mobile platform a full-size van had to be converted into a measurement vehicle as shown in Fig. 4.

By contrast, the setup used for taking measurements of impulsive noise in our study uses inexpensive components that can be acquired with the limited budget of an undergraduate research project, and consists of a Lime SDR platform from Lime Microsystems [8] along with an average laptop computer as seen in Fig. 5. We note that the Lime SDR can be configured as a generic, standalone I-Q receiver, while all of the other items (the logarithmic detector, the spectrum analyzer, and the digital oscilloscope) are integrated in the laptop software.

The Lime SDR has emerged as a competitive SDR platform in terms of its cost and user base, which have rapidly integrated it into the open-access SDR community. Similar to other SDR platforms (e.g. the HackRF [9] or the USRP Bus Series [10]) the Lime SDR connects with a host computer through a USB interface and features two independent transmit and receive paths, being capable of implementing complex applications that include WiFi repeaters, spread spectrum systems, or even MIMO applications. In terms of programming, the Lime SDR platform can be set up to as a standalone I-Q receiver using PothosWare [17], which is an open-source package specific to the Lime SDR that is based on GNURadio and streamlines its programming. The USB 3.0 interface of the Lime SDR platform with the host computer limits its supported bandwidth to 60 MHz baseband equivalent bandwidth, which translates to an effective I/Q bandwidth of 30 MHz. For our noise measurements a bandwidth of 10 MHz was sufficient and allowed us to set up the Lime SDR over legacy USB 2.0 interface. This way, our software setup can be ported to other SDR platforms like the HackRF or the USRP 1 that interface with the host computer over USB 2.0.

Our measurement setup, shown in Fig. 5, is highly portable and can be installed on a hand-pushed rolling cart for indoor measurements or in a small size vehicle for outdoor measurements. We note that no additional power supply is required, and a fully charged laptop battery easily allows 20-30 minute measurement runs as performed in our experiment. For our measurements we chose the 900 MHz frequency band for two main reasons, one of them being the fact that the default matching network on the RX1 L input of the Lime SDR is optimized for a good return loss at 900MHz. In addition, the 900 MHz band is a good candidate for background noise measurements since it is virtually free from continuous waveform (CW) carriers and interference in the environments selected for our measurements. The only exception is the residential neighborhood environment, where occasional frequency-hopping signals from smart meters in the 902 MHz band can be regarded as impulsive noise occurrences.

Because the noise figure of the Lime SDR is rather large (exceeding 10 dB), an Analog Devices AD 8353 amplifier was used to improve receiver sensitivity. This has a nominal gain of 20 dB with a noise figure of approximately 5.2 at 900 MHz, an input voltage

standing waveform ratio (VSWR) of 1.2 : 1. The amplifier was fitted in the custom enclosure built for the Lime SDR and was powered from a 3 V DC battery for mobile operation.

The antenna used to collect RF signals was a 1/4-wave monopole and was tested with a network analyzer, which revealed a reasonable response at the frequency of the lowest VSWR of 1.7:1 of 900 MHz. When combined with the AD 8353 amplifier the resulting VSWR of 1.2 : 1 mismatch error is bounded by a ±5% mismatch measurement error [18].

For programming, the SoapySDR interface of PothosWare [17] was used to set the parameters of the Lime SDR. This allows specification of the center frequency, sampling rate, RF gain values, and intermediate frequency (IF) output bandwidth of the Lime SDR using a single block element. The IF processing stage passes the wideband IF signal through a narrowband FIR filter with 250 kHz bandwidth chosen in anticipation of impulse durations and intervals on order 10^{-5} s (tens of microseconds) [5]. The filter taps were determined using the FIR designer included in PothosWare, and a Gaussian shape was also realized, thereby optimizing the transient impulse response. The resulting FIR filter, employing a Hanning windowing, with Gaussian response, and a gain of 20 dB required 31 taps.

The pre-filtered, undetected waveform is output to a display dashboard, which is shown in Fig. 6, and which includes a "waterfall" type spectrogram, a periodogram, and a time domain oscillograph display to visualize the temporal nature of the received signal and identify impulses. We note that, while useful to identify continuous waveform activity, the periodogram display also verifies the proper IF bandwidth shaping, and gives a measure of noise floor and LNA effectiveness. Furthermore, masking is provided for minimum/maximum power levels, which is especially useful for quick checks during mobile operation (accomplished while driving).

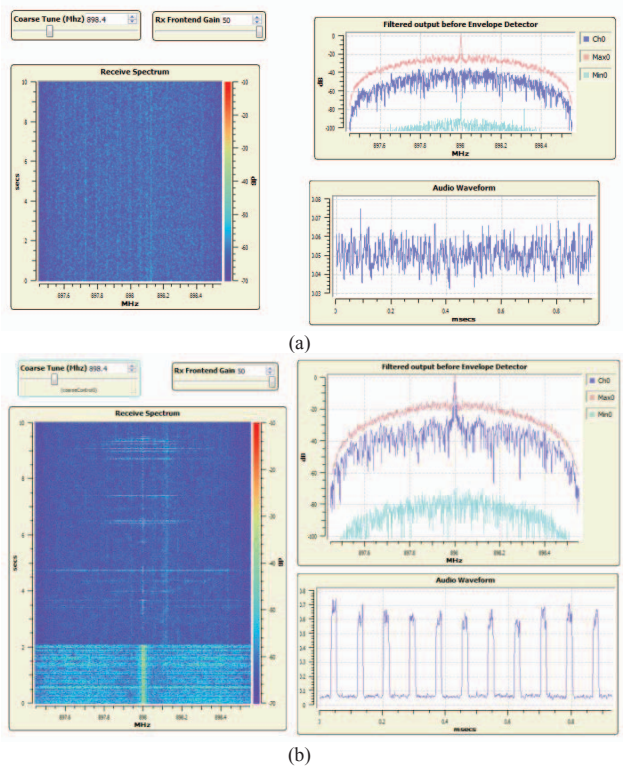

Fig. 6. PothosWare dashboard displaying the RF waterfall spectrogram, IF periodogram, and a waveform oscillograph for (a) Gaussian thermal noise and (b) broadband impulsive noise shower.

A power detection chain is included in the receiver to determine the root mean-squared (RMS) value of the received signal over the measurement interval. This value is also used as a checksum against the calculated value from the integrated PDF over the same measurement interval. An envelope detector block is also used to extract the signal magnitude. This is programmed to mimic an ideal diode in operation and employs a single-pole filter to achieve the detection. In Pothos/GNU Radio this is accomplished by using the linear recursive envelope follower routine, described by:

$$y(n) = (1 - \nu)|x(n)| + \nu y(n - 1) \qquad (3)$$

where ν is a constant that sets the tracking of $x(n)$ similar to how an RC filter sets the "following rate" of the conventional diode envelope detector. The value of ν is set by the user in Pothos, and for our measurements we took ν = 10 μs (which is equivalent to the duration of ten 10 MHz samples).

The envelope detector output, which is in the 32-bit IEEE floating-point representation, goes through additional processing that includes Gaussian shaping with a gain of 26 dB and decimation (by a factor of 10) to slow down the sample rate to provide time for subsequent processing of the measurements. This includes establishing the noise floor, which is necessary for subsequent normalization of the generated APD and for detecting impulsive noise instances. Using the noise floor value, thresholds are established by setting up five numerical bins in 6 dB increments, between 0 and 30 dB above the noise floor. Threshold detection produces binary signal ("1" or a "0") that depends on the instantaneous state of the input value relative to the threshold value; the binary threshold output signal is used to gate a 1 MHz clock, synchronous to all thresholds, which is integrated over a one-minute measurement interval resulting in a 32-bit float that represents a full-scale count, while retaining a dynamic range of 108 resolution. Data is then conditioned and normalized, followed by application of the $\log_{10}(\cdot)$ and storing in a compact data file in CSV format that is compatible with Matlab or other graphing software.

IV. Numerical Results

Once the Lime SDR is tethered to the laptop and the receiver configuration loaded to the SDR FPGA, operation is quite simple. As configured, the APD is generated at one minute intervals, and creates a new data file for each "start" operation. Before leaving the lab, a power calibration was performed to establish the noise floor, as well as linearity over a 30 dB region. The noise floor was determined to be –116 dBm (measured with an Agilent E4432B RF signal source), with less than 0.5 dB of total linear discrepancy. This value is consistent with expected value of thermal noise [2], kTB, which for oper-

[2] Thermal noise value is kTB, where k = 1.38 × 1023 J/K is Boltzman's constant, T is the operating temperature of the system in K, and B is the receiver bandwidth.

ating temperature of 300 K and RF bandwidth equal to 250 kHz is around –119 dBm. Output waveforms for zero-input settled around 30 mV RMS, which is the value used for threshold-above noise floor determination. Prior to each run, a 50 Ω termination was placed at the LNA input to verify the –116 dBm noise floor and to watch for any APD activity (none was expected since a standard deviation of the noise of 5 mV is far less than the 6 dB step size of the first bin). The antenna was then attached, and the receiver re-started to reset all counters, and overwrite (hence creating) a new output file. Fig. 6 demonstrates received signals for thermal Gaussian noise (on a 50 Ω load) as well as an instance of an actual impulsive shower activity at one of the measurement locations.

A. APDs

APD data was collected for three specific RF environments in Newport News, VA, that included a typical office workspace (at Jefferson Lab), a hospital campus (Riverside Medical Center), and a commute from a busy urban location to a residential destination (from Jefferson Lab to the Hilton Village neighborhood), and results obtained are shown in Fig. 7. In each case, preliminary runs were performed to identify any CW activity or anomalous behavior from the environment or the SDR, followed by generation of APDs for each of these scenarios. From Fig. 7 we note that significant ambient power levels are present, displaying values of 30 dB above thermal noise floor for significant periods. In all scenarios, the elevated Gaussian-like APDs are the result of multiple independent sources of impulsive noise that combine according to the Central Limit Theorem. Impulsive activity is especially apparent for office environment, where steep changes in the APDs are noticeable, indicate highly-impulsive behavior due to isolated impulsive noise sources.

B. Middleton Class A Noise Model Parameters

While APD plots provide a qualitative description of the RF environment, determining the parameters of the underlying Middleton model for Class A impulsive noise is also important since these parameters can also be used in assessing link performance through metrics such as the bit error rate (BER). Furthermore, the time evolution of the APDs, which is also evidence of the non-stationary nature of the impulsive noise, is most evident when the values of the impulsive index A and of the intensity index Γ of the Middleton Class A model in equations (1) and (2) are tracked. These parameters are extracted from the measured data off-line by implementing the approach in [11], [13].

The first step in the empirical characterization of the impulsive noise parameters A and Γ is determining the RMS value of the measured noise signal, which is required to normalize the APD before parameter extraction. This is obtained through off-line processing of the APD data using cubic spline interpolation on the APD data and is shown in Fig. 8, in which the calculated and measured noise values are compared. In most cases, the difference was within ±0.5 dB, which implies an error of about 6%, and good agreement is shown for lower power levels with moderately Gaussian conditions. However, large signal levels (30 dB above noise floor) resulted in larger discrepancies, making the interpolation process more difficult. This was the case especially with measurements taken in the commuter scenario shown in Fig. 8(b), which illustrates the tendency of the cubic spline interpolation to overfit data, resulting in higher RMS values than the measured ones.

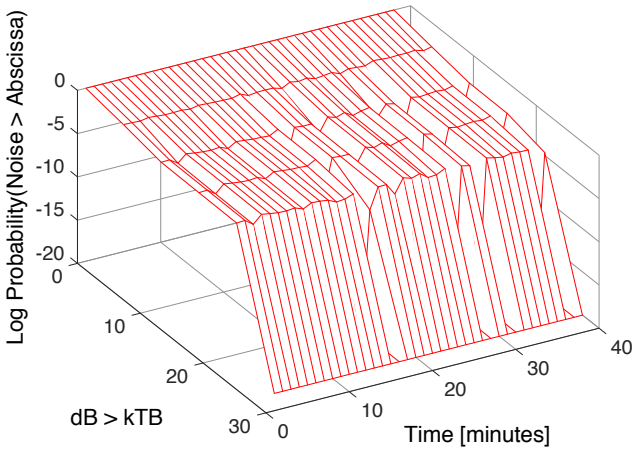

(a)

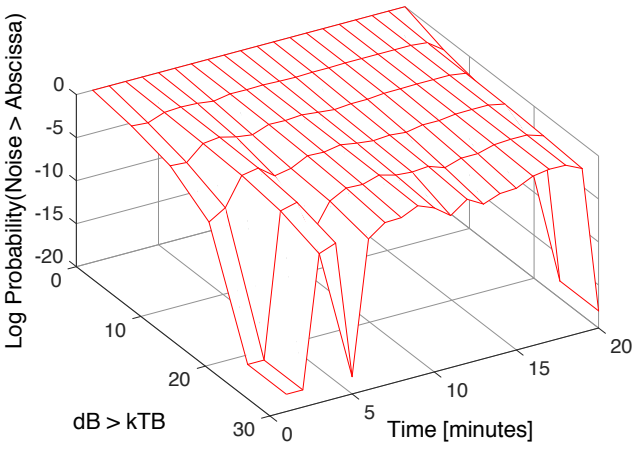

(b)

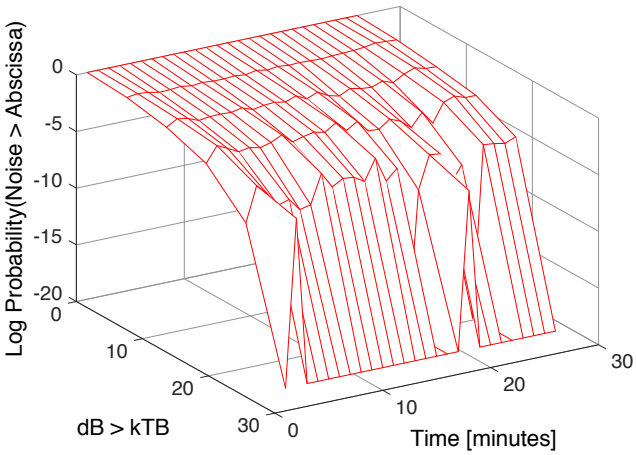

(c)

Fig. 7. Time evolution of APD statistics for (a) medium-density office workspace environment, (b) urban commute scenario, and (c) hospital campus. X-axis represents time (in minutes), Y-axis represents the threshold bins above noise floor (in 6 dB increments), and Z-axis is the log-probability.

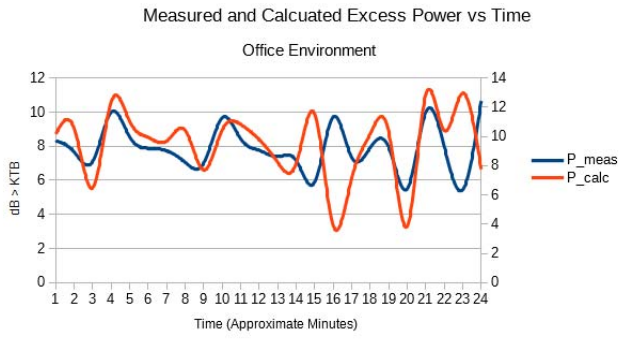

(a)

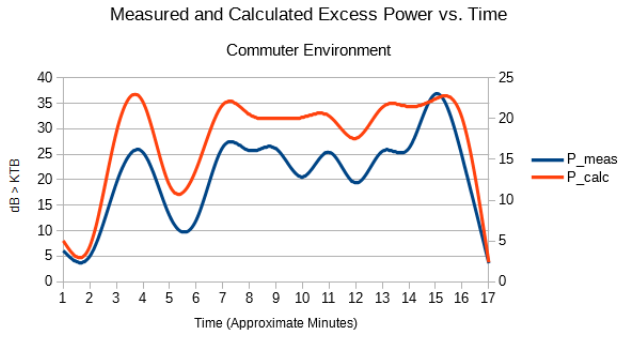

(b)

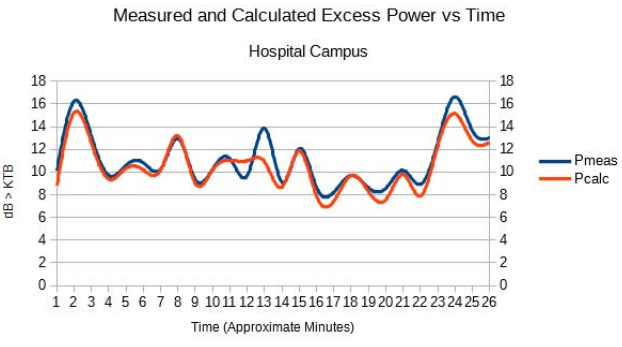

(c)

Fig. 8. Measured and calculated excess power levels (above thermal noise floor) for a) medium-density office workspace environment, (b) urban commute scenario, and (c) hospital campus.

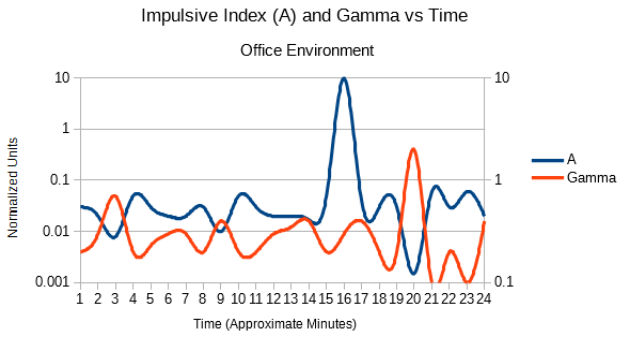

(a)

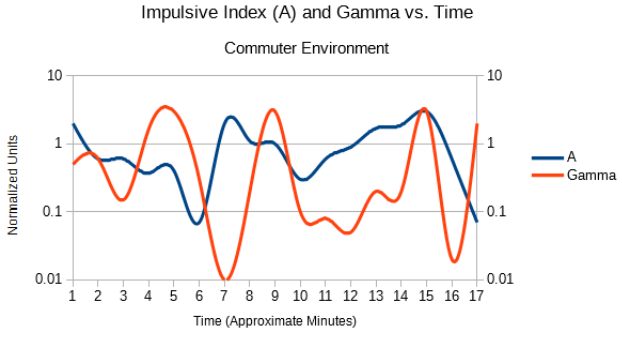

(b)

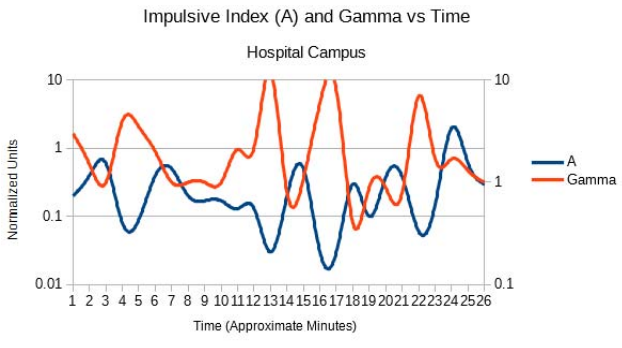

(c)

Fig. 9. Measured and calculated excess power levels (above thermal noise floor) for a) medium-density office workspace environment, (b) urban commute scenario, and (c) hospital campus.

The time variation of the impulsive index A and of the intensity index Γ corresponding to the three measurement scenarios obtained using the measurement data is shown in Fig. 9, where values less than 1 for each parameter indicate impulsive behavior, while values larger than 1 correspond to Gaussian statistics. From Fig. 9, we note that each scenario displays significant variation of one or both indices that can extend over two orders of magnitude or even more, with office and commute scenarios being appearing more impulse-dominated (indices are more frequently below 1), while the hospital scenario displays a more Gaussian behavior with indices values exceeding 1 only in a few instances. These results are consistent with what the spectrogram waterfall plot displayed during the measurements, when bursts and even showers of impulsive activity were detected, followed by intervals when only thermal noise would be detected. For the commute scenario, known power line "hot spots" appear to emit RF as a distributed source, which, when combined with random delays at the antenna, resemble highly elevated thermal noise levels (as high as 30 dB above noise floor), with a marked tail-off at the 15-minute mark, which corresponds to a wooded residential area with no known RF or industrial activity other than smart meters in homes.

V. Discussion and Conclusion

In this paper we presented a study demonstrating the utility of SDR platforms for taking noise measurements and evaluating statistical parameters for impulsive noise models. The specific application presented in the paper focuses on a narrowband system with RF bandwidth of 250 kHz operating in the 900 MHz band, but can be easily adapted to other applications due to the versatility of the SDR platforms. Since the Lime SDR operates over a wide

range of frequencies, covering the HF, VHF and UHF bands up to 3.8 GHz, with an RF bandwidth of up to 80 MHz, the measurement setup requires minimal software changes to be applied to impulsive noise measurements and characterization in other scenarios. For example, the system presented in the paper may be used to complement the numerical simulation results in [19] with actual RF measurements of the noise radiated by a microwave oven over a narrowband channel with 300 kHz bandwidth at 2 GHz similar to the one in [20]. Alternatively, the system can be used for characterization of wideband UHF digital TV channels with a bandwidth of 10 MHz in the 700 MHz band [21].

While the study presented in the paper uses the Lime SDR in receive mode to collect actual measurements of impulsive noise, this can also be used in transmit mode to synthesize impulsive noise signals using computer generated I and Q components [22]. We note that accomplishing this requires in essence developing the software for generating the I and Q components of the artificial impulsive noise along with programming the Lime SDR to transmit it over the frequency band of interest, and can be useful for testing purposes in a lab setup.

From a practical perspective, the presented approach allows RF site-surveyors to accumulate noise data and to identify best and worst-case noise scenarios by using lightweight and highly portable battery-powered equipment, and can be easily adapted to perform measurements of broadband or narrowband electromagnetic interference emissions. Usually, these are performed by nationally recognized testing laboratories, and can be both expensive and time consuming, since they require specialized personnel and test fixtures, hours of calibration, and lengthy measurements, to produce highly accurate certified results. However, when stringent accuracy and certification are not absolutely necessary, as may be the case with consumer-type applications, taking advantage of the versatility of SDR platforms, to establish dedicated systems for electromagnetic compatibility testing can significantly reduce cost, while still providing useful information for system design.

In future studies, we plan to investigate application of machine learning and artificial intelligence techniques to processing large amounts of noise measurement data, which could result in faster data processing and extraction of the relevant noise parameters.

Acknowledgment

The authors would like to acknowledge the Technical Editor, Prof. Kye Yak See, as well as the anonymous reviewers, for their comments and suggestions on improving the presentation of this work.

References

1. J. J. Lemmon, "Wideband Model of Man-Made HF Noise and Interference," Radio Science, vol. 32, no. 2, pp. 525–539, March-April 1997.
2. L. R. Espeland and A. D. Spaulding, "Amplitude and Time Statistics for Atmospheric Radio Noise," Environmental Science Services Administration, ESSA Technical Memorandum ERLTM-ITS 253, September 1970.
3. "URSI Special Report No. 7 on the Measurement of Characteristics of Terrestrial Radio Noise," International Union of Radio Science, Tech. Rep., 1962.
4. K. Furutsu and T. Ishida, "On the Theory of Amplitude Distribution of Impulsive Random Noise," Journal of Applied Physics, vol. 32, no. 7, pp. 1206–1221, July 1961.
5. J. Musson, "Man-made Impulsive Noise on the 137 MHz VHF LEOSAT Channel," Master's thesis, Virginia Polytechnic Institute and State University, Department of Electrical and Computer Engineering, 1994, thesis director: Prof. T. Pratt.
6. G. Kolumban, T. I. Krebesz, and F. C. M. Lau, "Theory and Application of Software Defined Electronics: Design Concepts for the Next Generation of Telecommunications and Measurement Systems," IEEE Circuits and Systems Magazine, vol. 12, no. 2, pp. 8–34, Second quarter 2012.
7. W. H. W. Tuttlebee, "Software Defined Radio: Facets of a Developing Technology," IEEE Personal Communications Magazine, vol. 6, no. 2, pp. 13–18, April 1999.
8. Lime Microsystems, "LimeSDR," https://limemicro.com/products/boards/limesdr/, accessed: Feb. 18, 2019.
9. Great Scott Gadgets, "HackRF One. An Open Source SDR Platform," https://greatscottgadgets.com/hackrf/, accessed: Feb. 18, 2019.
10. Ettus Research, "USRP Bus Series Products," https://www.ettus.com/product/category/USRP-Bus-Series, accessed: Feb. 18, 2019.
11. D. Middleton, "Canonical Non-Gaussian Noise Models: Their Implications for Measurement and for Prediction of Receiver Performance," IEEE Transactions on Electromagnetic Compatibility, vol. EMC-21, no. 3, pp. 209–220, August 1979.
12. ——, "Non-Gaussian Noise Models in Signal Processing for Telecommunications: New Methods and Results for Class A and Class B Noise Models," IEEE Transactions on Information Theory, vol. 45, no. 4, pp. 1129–1149, May 1999.
13. ——, "Procedures for Determining the Parameters of the First-Order Canonical Models of Class A and Class B Electromagnetic Interference [10]," IEEE Transactions on Electromagnetic Compatibility, vol. EMC- 21, no. 3, pp. 190–208, August 1979.
14. D. C. Popescu, J. Musson, and O. Popescu, "Empirical Characterization of Man-Made Impulsive Noise Using Open-Source Software Defined Radio Platforms," in Proceedings 14th IEEE International Symposium on Signals, Circuits, and Systems – ISSCS 2019, Iasi, Romania, July 2019.
15. D. Middleton, "Statistical-Physical Models of Urban Radio-Noise Environments - Part I: Foundations," IEEE Transactions on Electromagnetic Compatibility, vol. EMC-14, no. 2, pp. 38–56, May 1972.
16. ——, "Statistical Models of Electromagnetic Interference," IEEE Transactions on Electromagnetic Compatibility, vol. EMC-19, no. 3, pp. 106– 127, August 1977.
17. J. Blum, "PothosWare," http://www.pothosware.com/, accessed: Feb. 18, 2019.
18. I. A. Harris and F. L. Warner, "Reexamination of Mismatch Uncertainty When Measuring Microwave Power and Attenuation," IEE Proceedings H - Microwaves, Optics and Antennas, vol. 128, no. 1, pp. 35–41, February 1981.
19. S. Miyamoto, M. Katayama, and N. Morinaga, "Performance Analysis of QAM Systems Under Class A Impulsive Noise Environment," IEEE Transactions on Electromagnetic Compatibility, vol. 37, no. 2, pp. 260– 267, 1995.
20. ——, "Receiver Design Using the Dependence Between Quadrature Components of Impulsive Radio Noise," in Proceedings 1995 IEEE International Conference on Communications (ICC), vol. 3, Seattle, WA, June 1995, pp. 1784–1789.
21. M. G. Sanchez, L. de Haro, M. C. Ramon, A. Mansilla, C. M. Ortega, and D. Oliver, "Impulsive Noise Measurements and Characterization in a UHF Digital TV Channel," IEEE Transactions on Electromagnetic Compatibility, vol. 41, no. 2, pp. 124–136, 1999.
22. P. Torio, M. G. Sanchez, and I. Cuinas, "An Algorithm to Simulate Impulsive Noise," in Proceedings 19th IEEE International Conference on Software, Telecommunications and Computer Networks (SoftCOM), Dubrovnic, Croatia, September 2011.

Biographies

Otilia Popescu *(M'04—SM'10) received the Engineering Diploma with specialization in electrical and computer engineering from Polytechnic Institute of Bucharest, Romania, and the Ph.D. degree also in electrical and computer engineering from Rutgers University, New Brunswick, NJ. Her research interests*

are in the areas of wireless communication systems, wireless networking, and engineering education. Dr. Otilia Popescu is currently working as Associate Professor in the Department of Engineering Technology at Old Dominion University, Norfolk, VA, where she is also the Director of the Electrical Engineering Technology Program. She is a senior member of IEEE and a member of the American Society for Engineering Education (ASEE), and she has served as associate editor for IEEE Communications Letters (2014-2019). In addition, she is an active member of the technical program committee for several IEEE international conferences including GLOBECOM, ICC, and WCNC conferences.

John Musson *received the B.S. degree in physics from Michigan State University, East Lansing, MI, and M.S. degree in electrical engineering from Virginia Polytechnic Institute and State University, Blacksburg, VA. He is currently a Ph.D. candidate in the Department of Electrical and Computer Engineering, Old Dominion University, Norfolk, VA, working on research in the area of superconductive thin films. He is currently working in the Engineering Division at Thomas Jefferson National Accelerator Facility (JLAB), in Newport News, VA, focusing on beam diagnostics, RF control systems, instrumentation, and superconducting RF cavity development for JLAB's 12 GeV Continuous Electron Beam Accelerator Facility (CEBAF).*

Dimitrie C. Popescu *(M'02, SM'05) received the Engineering Diploma with specialization in electrical and computer engineering from Polytechnic Institute of Bucharest, and the Ph.D. degree also in electrical and computer engineering from Rutgers University. He is a Professor in the Department of Electrical and Computer Engineering, Old Dominion University, Norfolk, Virginia, where he has been since 2006. His research interests are in the areas of wireless communication systems and include spectrum sensing and modulation classification, dynamic spectrum access for cognitive radios, transmitter/receiver optimization to support quality of service, software defined radios, and vehicular networking. Dr. Dimitrie Popescu is a Senior Member of the IEEE and serves as an associate editor for IEEE Open Journal of the Communications Society and for Elsevier Computer Communications Journal. He has also served as associate editor for IEEE Transactions on Wireless Communications (2014-2019) and for IEEE Communications Letters (2010-2014). In addition, he is active in the technical program and organizing committees for the IEEE Global Telecommunications Conference (GLOBECOM), the IEEE International Conference on Communications (ICC), the IEEE Wireless Communications and Networking Conference (WCNC), and the IEEE Vehicular Technologies Conference (VTC).* **EMC**

CALL FOR AUTHORS

PROJECT: EMC Theory and Practice

DESCRIPTION: For this project, EMC Theory and Practice, a book has a combination of the following features: 1) fundamental theories and/or applications of EMC, 2) advance the areas of knowledge in EMC, and 3) audience is a practicing EMC engineer and/or EMC researcher, educator.

PUBLISHER: Wiley-IEEE Press

SPONSORSHIP: IEEE EMC Society

TARGETED PUBLICATION DATE: 2021 and forwards

COMPENSATION: Royalties paid to author(s) directly

REQUIREMENTS: Present or past expertise(s) in an EMC discipline. Willingness to write a high-quality technical contribution with personal commitment to schedules and deadlines.

RESPONSES DUE DATE: Applications accepted on an ongoing basis.

FORMAT OF RESPONSES: Name, affiliation, contact information, one paragraph of background information concerning your capabilities, title of contribution (see "EMC Subject Areas of Interest" below) and a brief description of the contribution.

EMC SUBJECT AREAS of INTEREST: Please provide a title for your book whose subject matter falls within one or more of the following areas of interest: 1) EMC Theories and Practice, 2) Mobile Systems, 3) Power and Energy, 4) Biomedical, Biotech, Healthcare, 5) EMC Standards, 6) EDA Applications, 7) Signal and Power Integrity, 8) Testing Techniques and Methods, 9) Testing Facilities, 10) Mobile and Wireless Communications, 11) Autonomous Systems, 12) High Power Electromagnetics, 13) EMC Management, 14) EMC Education and Training.

CONTACT INFORMATION

Ray Perez, Wiley-IEEE Press Liaison for the IEEE EMC Society

email: reyjperez@msn.com